

## Supporting Information

### **Continuous Heat Harvesting by An Ionogel Mixed with PEDOT:PSS under Both Fluctuated and Steady Temperature Gradients**

Yu Wu,<sup>a,b</sup> Qi Qian,<sup>a,b</sup> Cheng Xu,<sup>a</sup> Zhijun Chen,<sup>a</sup> Kun Zhang,<sup>a</sup> Xinran Du<sup>a</sup> and Jianyong Ouyang<sup>a,b,\*</sup>

<sup>a</sup> Department of Materials Science and Engineering, National University of Singapore, 117574, Singapore

<sup>b</sup> National University of Singapore (Suzhou) Research Institute, No. 377 Linqun Street, Suzhou Industrial Park, Suzhou, Jiangsu 215123, China

E-mail: [mseoj@nus.edu.sg](mailto:mseoj@nus.edu.sg) (J. Ouyang)

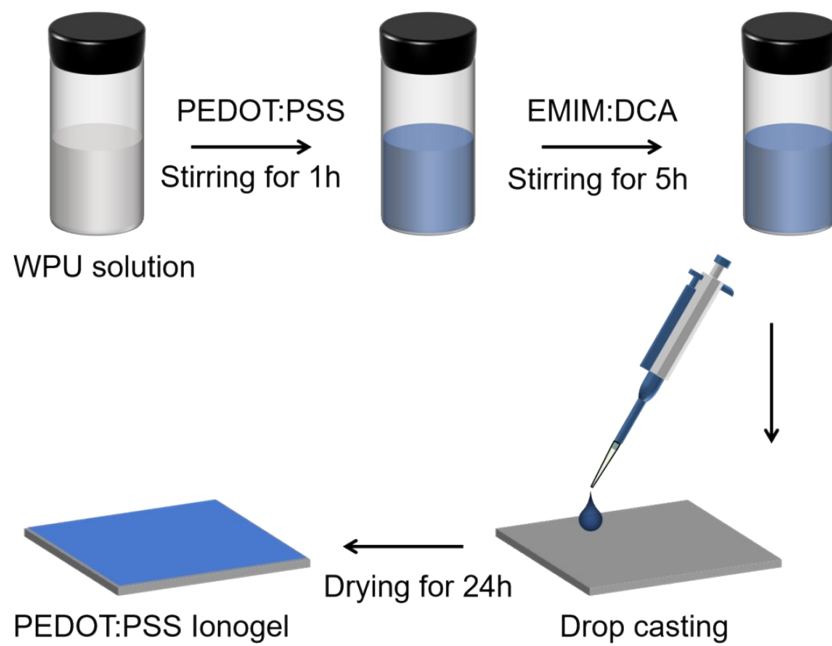


**Fig. S1.** Schematic illustration for the preparation of PEDOT:PSS ionogels.

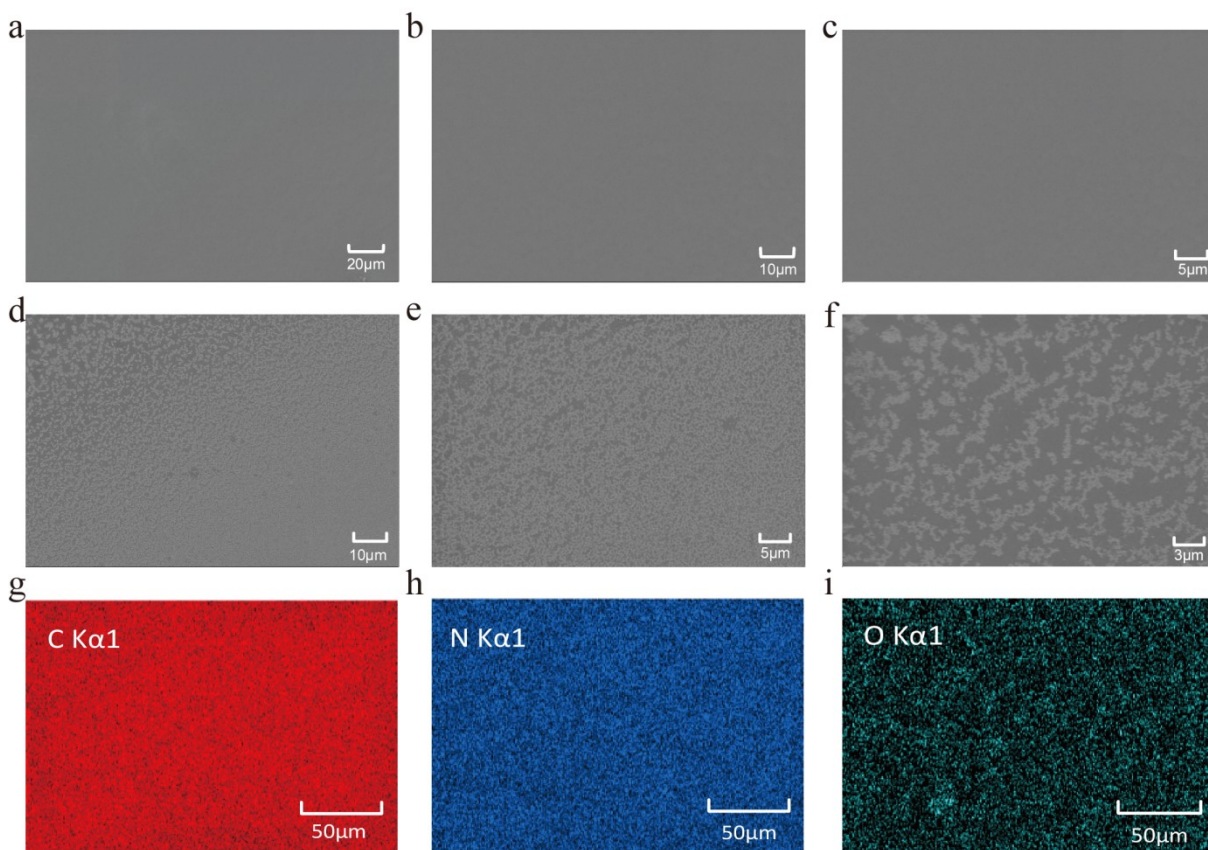


**Fig. S2.** SEM images of PEDOT:PSS ionogels with the PEDOT:PSS loadings of (a-c) 0 and (d-f) 5 wt.%. EDS mappings of (g) the C, (h) N, and (i) O elements of ionogels with the PEDOT:PSS loading of 5 wt.%.

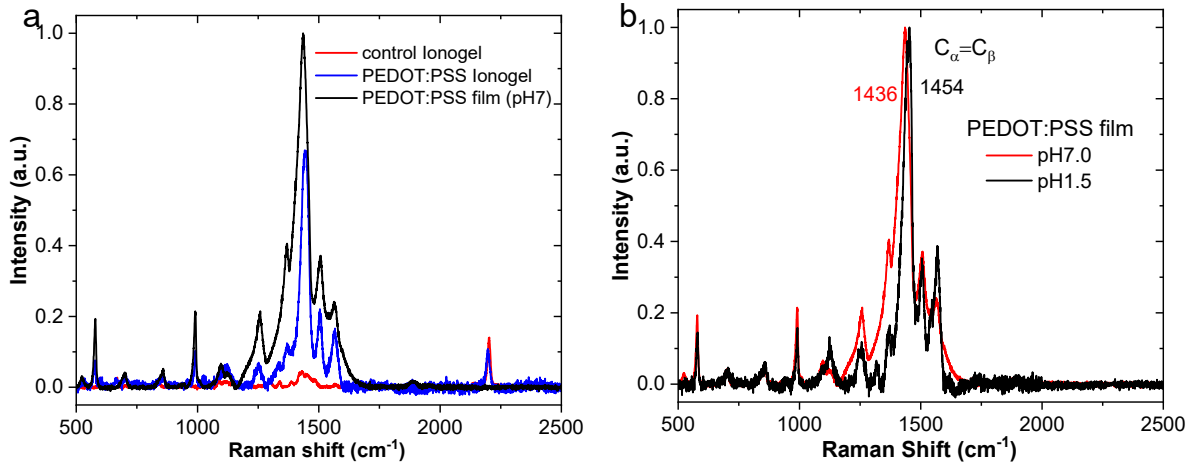


**Fig. S3.** Raman spectra of (a) a control ionogel without PEDOT:PSS, a PEDOT:PSS ionogel and a PEDOT:PSS film and (b) PEDOT:PSS films prepared from PEDOT:PSS aqueous dispersions with the pH values of 1.5 or 7.

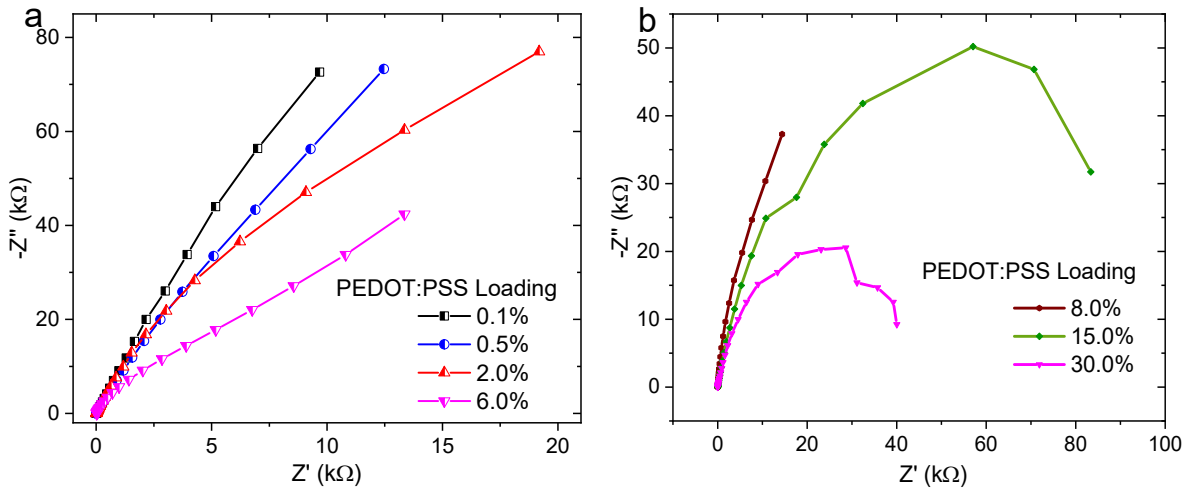


**Fig. S4.** Nyquist plots of ionogels with the PEDOT:PSS loadings of (a) 0.6 wt%-6.0 wt.%, and (b) 8.0 wt.-30.0 wt.%.

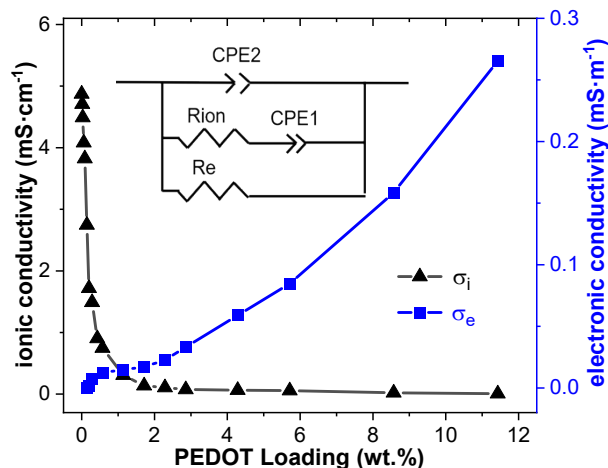


**Fig. S5.** Variations of the ionic and electronic conductivities of the ionogels with the PEDOT loading in the PEDOT:PSS ionogels.

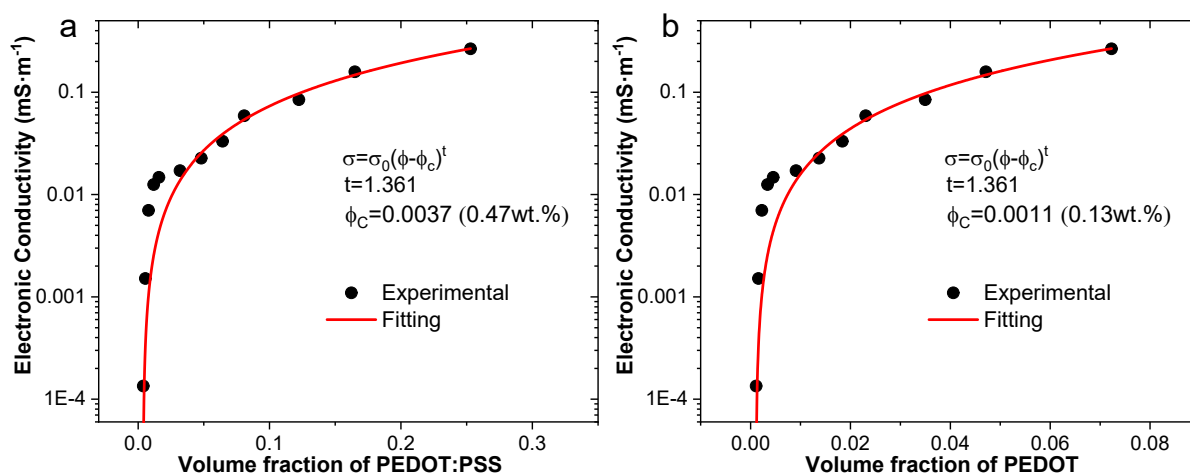


**Fig. S6.** Analyses of the dependences of the electronic conductivity of the PEDOT:PSS ionogels on (a) the PEDOT:PSS volume fraction and (b) PEDOT volume fraction excluding PSS/PSSH by the percolation model. The densities are  $1.5 \text{ g}\cdot\text{cm}^{-3}$ ,  $1.25 \text{ g}\cdot\text{cm}^{-3}$ , and  $1.1 \text{ g}\cdot\text{cm}^{-3}$  for PEDOT:PSS, WPU, and EMIM:DCA, respectively. The mass ratio of PSS<sup>-</sup> to PEDOT is 2.5.<sup>1,2</sup>

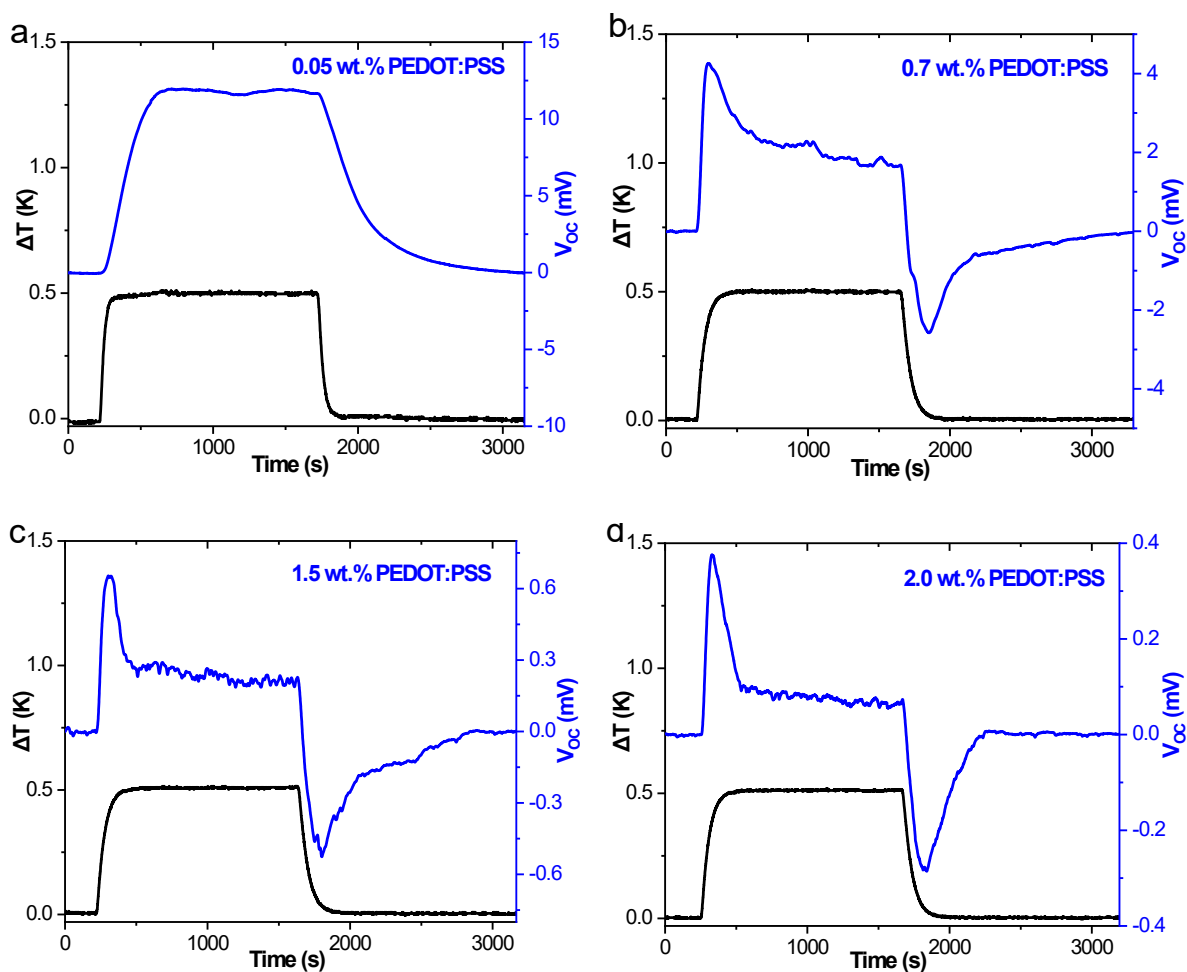


**Fig. S7.** Open-circuit voltage ( $V_{oc}$ ) profiles of the ionogels with the PEDOT:PSS loadings of (a) 0.05 wt.%, (b) 0.7 wt.%, (c) 1.5 wt.%, and (d) 2.0 wt.%.

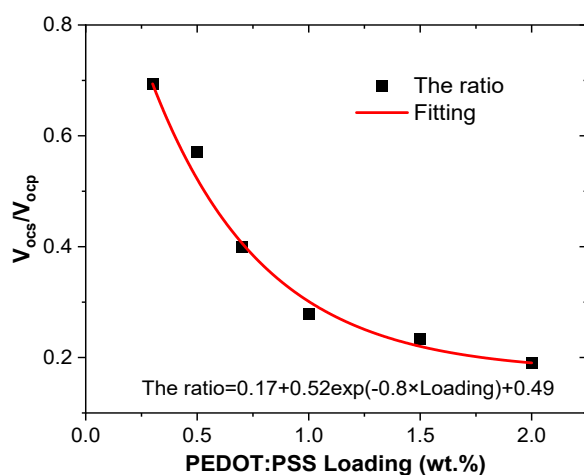


**Fig. S8.** Variation of the ratio of the steady open-circuit thermovoltage ( $V_{ocs}$ ) to the peak open-circuit thermovoltage ( $V_{ocp}$ ) with the temperature gradient. The solid curve is the fitting of the experimental results with an exponential decay function.

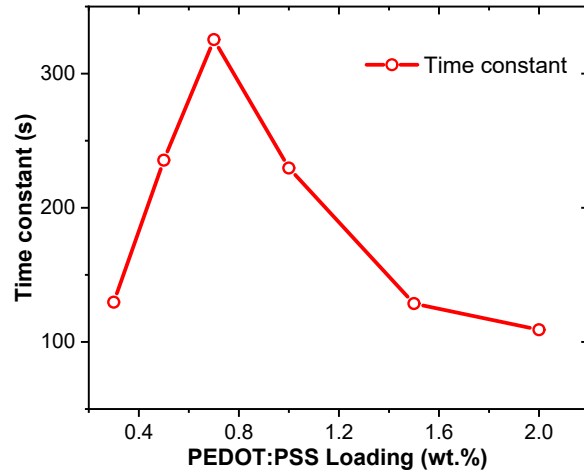


**Fig. S9.** Variation of the time constant ( $\tau$ ) with the PEDOT:PSS loading. The time constants were obtained by fitting the  $V_{oc}$  decays at the stage II with the exponential decay function,  $V_{oc} = V_0 e^{-(t-t_0)/\tau} + V_{ocs}$ .

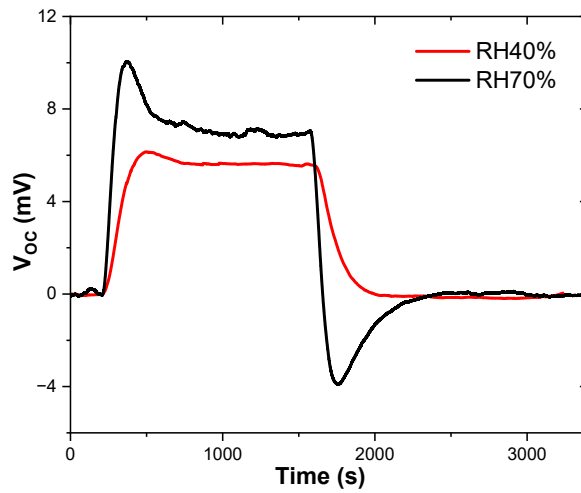


**Fig. S10.**  $V_{oc}$  profiles of PEDOT:PSS ionogels tested under different RHs. The PEDOT:PSS loading is 0.3 wt.% in the ionogels.

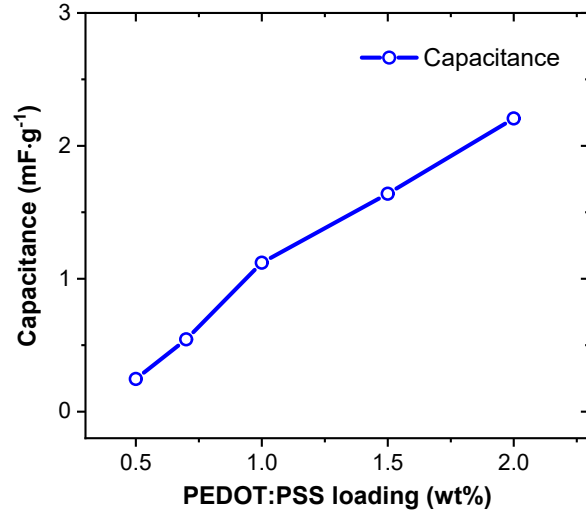


**Fig. S11.** Variation of the capacitance with the PEDOT:PSS loading. The capacitances were calculated in term of  $C = \tau/R_e$  at the stage II. The  $R_e$  values were calculated from the electronic conductivities of ionogels, and the  $\tau$  values were estimated by fitting the  $V_{oc}$  decay curves at the stage II.

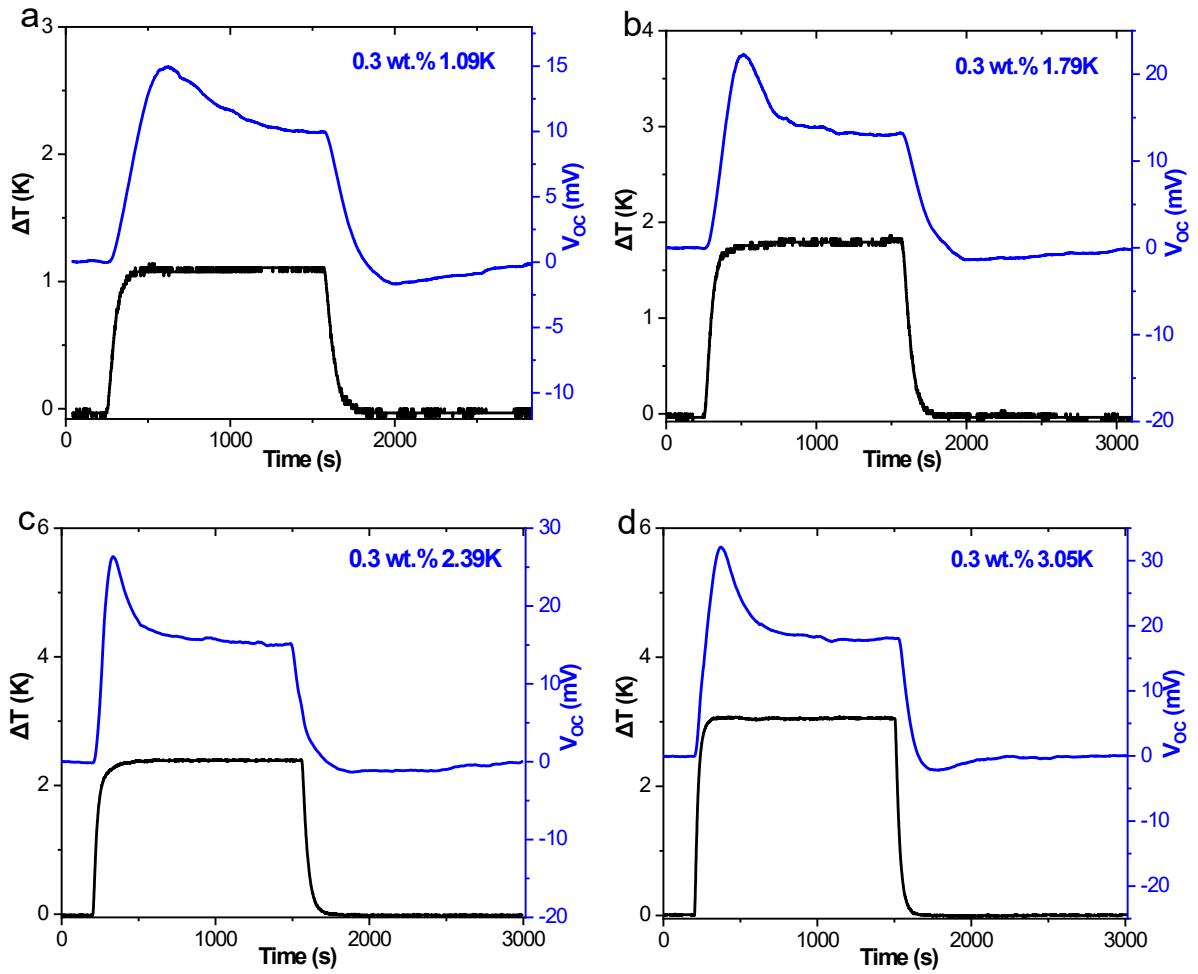


**Fig. S12.** Open-circuit voltage ( $V_{oc}$ ) profiles of PEDOT:PSS ionogels under the temperature gradients of (a) 1.09, (b) 1.79, (c) 2.39, and (d) 3.05 K. The PEDOT:PSS loading is 0.3 wt%.

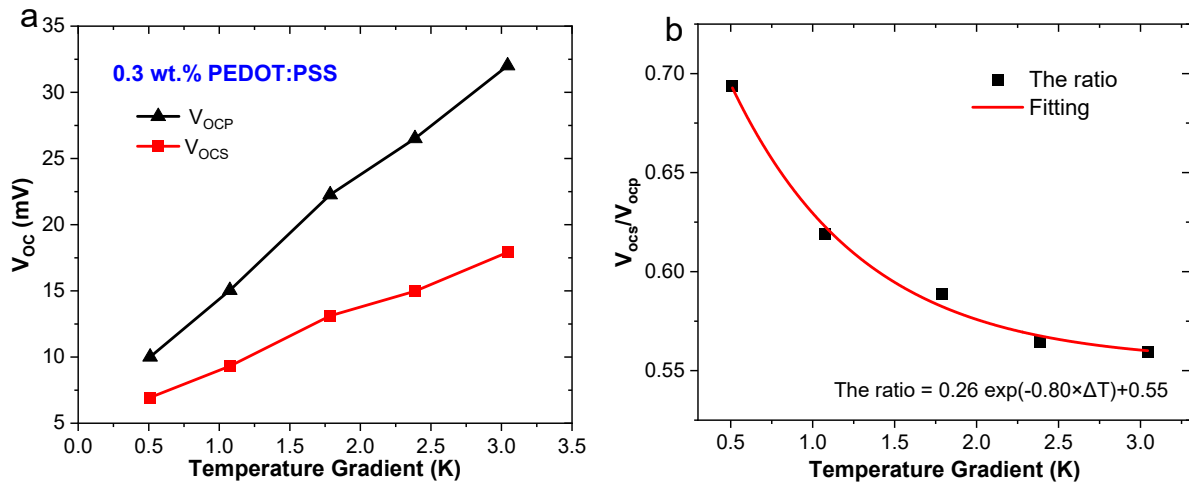


**Fig. S13.** Variations of (a) the peak open-circuit thermovoltage ( $V_{ocp}$ ) and steady open-circuit thermovoltage ( $V_{ocs}$ ) and (b) the ratio of the steady voltage to the peak voltage ( $V_{ocs}/V_{ocp}$ ) with the temperature gradient. The PEDOT:PSS loading of the Ionogel is 0.3 wt.%.

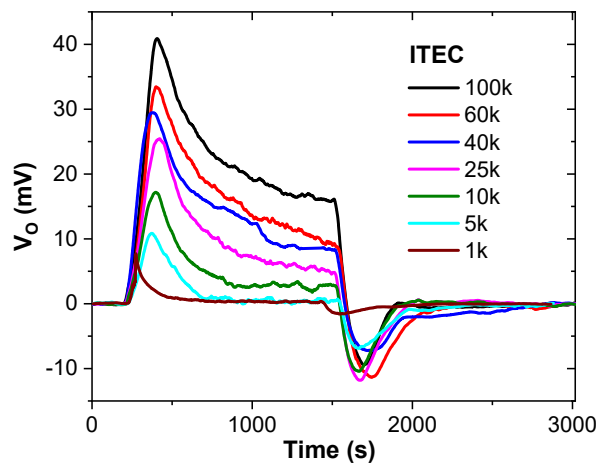


**Fig. S14.** Output voltage ( $V_o$ ) profiles on the external load with different resistances, which is connected to a control ITEC with no PEDOT:PSS.

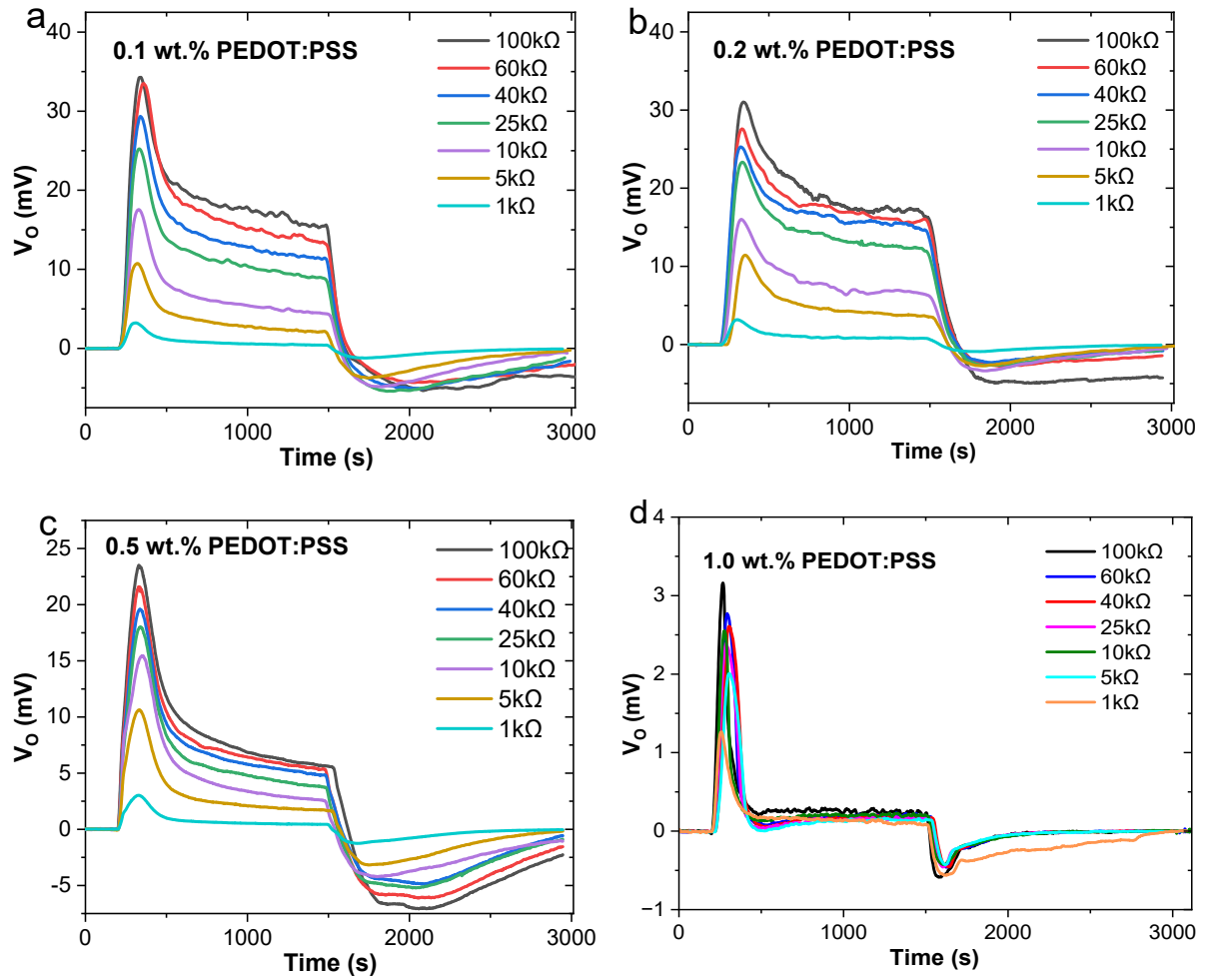


**Fig. S15.** Output voltage ( $V_o$ ) profiles on the external load with different resistances, which is connected to a MTEG with the PEDOT:PSS loadings of (a) 0.1 wt.%, (b) 0.2 wt.%, (c) 0.5 wt.%, or (d) 1.0 wt.%.

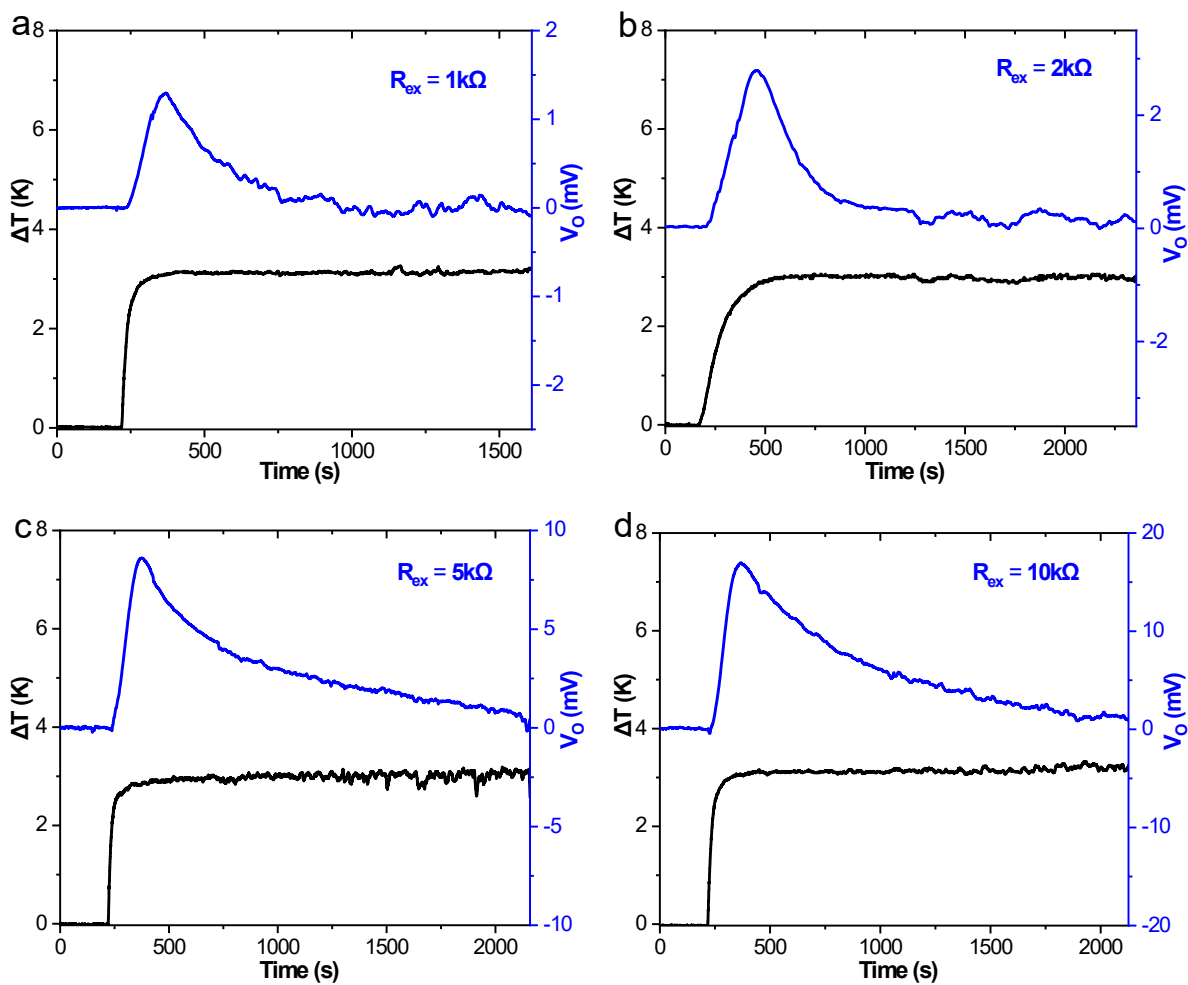


**Fig. S16.** Evolutions of the output voltages ( $V_o$ ) on the external load connected to a control ITEC without PEDOT:PSS over time. The external resistances were (a) 1 k $\Omega$ , (b) 2 k $\Omega$ , (c) 5 k $\Omega$ , and (d) 10 k $\Omega$ .

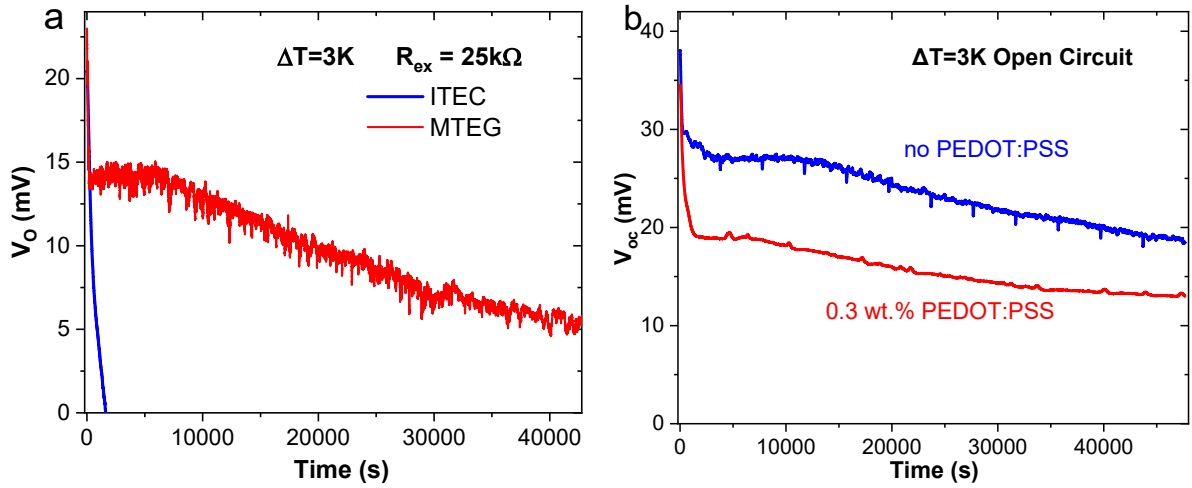


**Fig. S17.** (a) Evolution of the output voltage ( $V_o$ ) on the external load of 25 k $\Omega$  over time. The external load was connected to a control ITEC or an MTEG with the PEDOT:PSS loading of 0.3 wt% under the temperature gradient of 3 K. (b)  $V_{oc}$  evolution of the ionogels with the PEDOT:PSS loading of 0% or 0.3 wt% under the temperature gradient of 3 K.

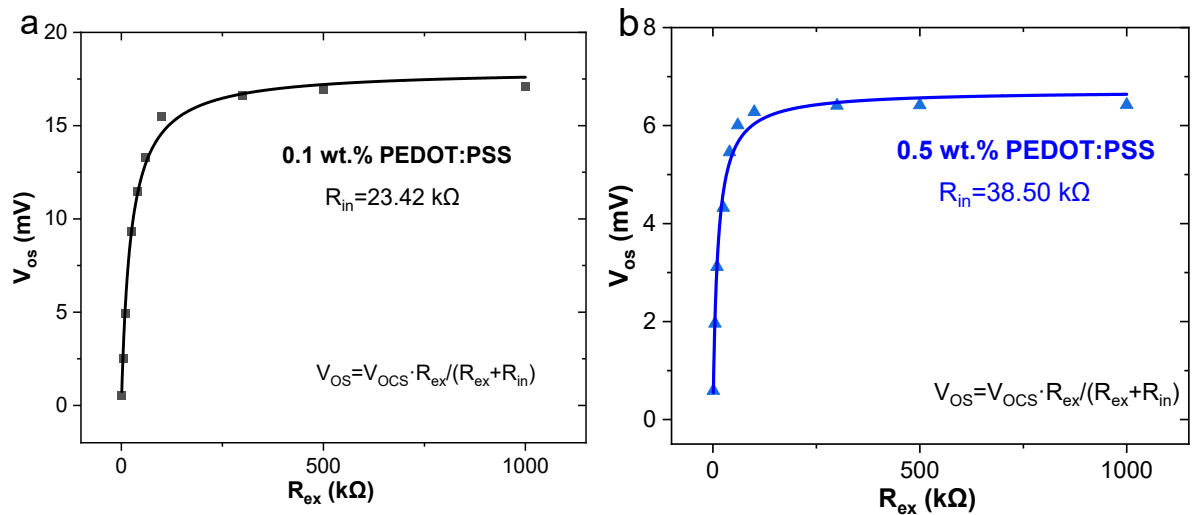


**Fig. S18.** Variations of steady output voltages ( $V_{os}$ ) with the external resistance ( $R_{ex}$ ) for the MTEGs with the PEDOT:PSS loadings of (a) 0.1 wt.% and (b) 0.5 wt.%.

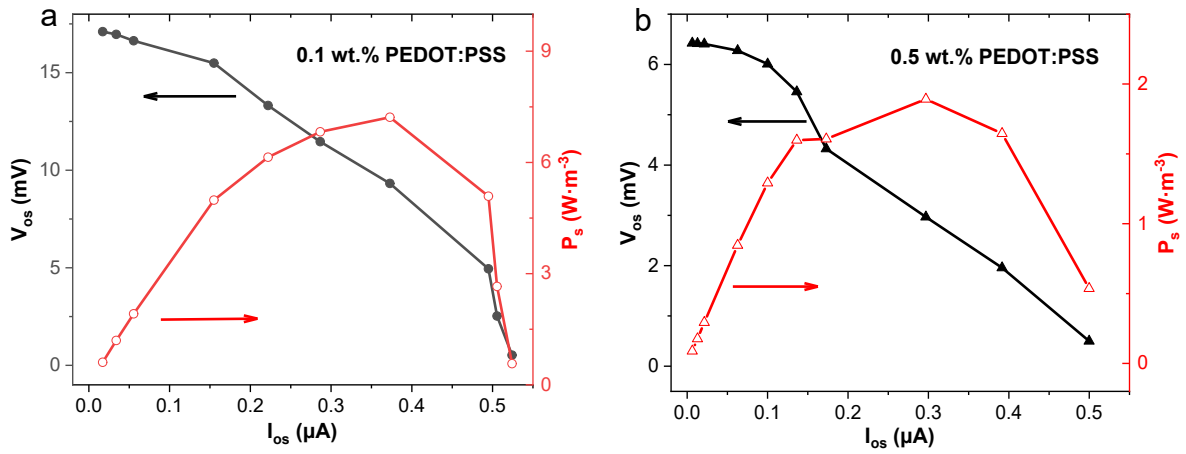


**Fig. S19.** Dependences of the steady output voltages ( $V_{os}$ ) and steady output power densities ( $P_s$ ) on the steady output current ( $I_{os}$ ) for the MTEGs with the PEDOT:PSS loadings of (a) 0.1 wt.% and (b) 0.5 wt.%.

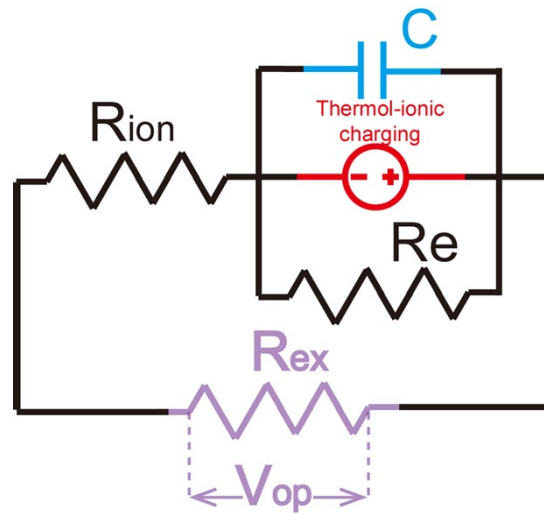


**Fig. S20.** Equivalent circuit for a MTEG connected with an external load.

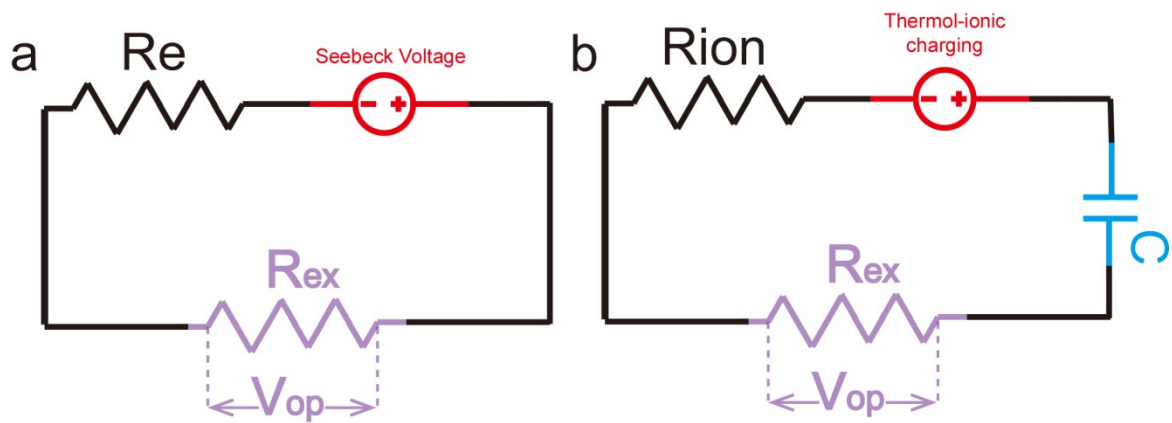


**Fig. S21.** Equivalent circuits for (a) an ITEC and (b) a TEG connected with an external load.

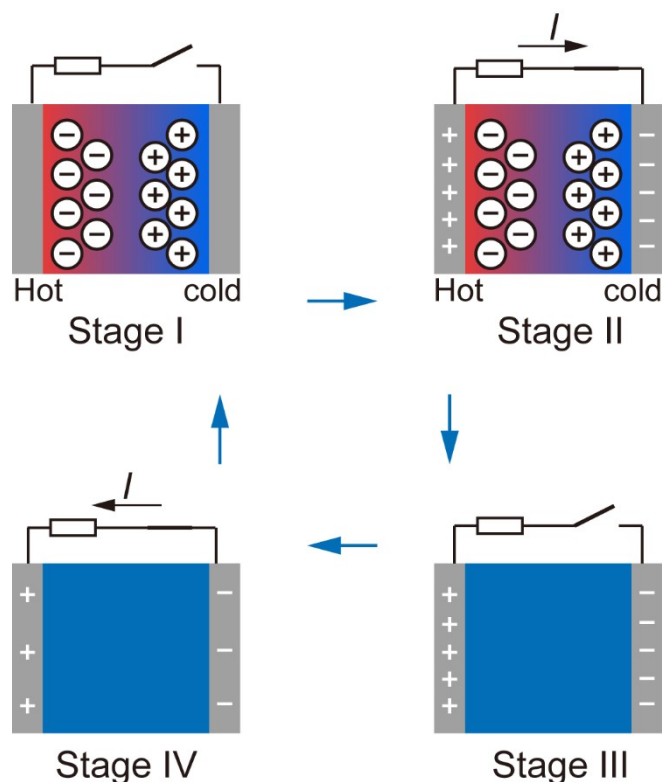


**Fig. S22.** Schematic illustration of the working principle of an ionic thermoelectric capacitor (ITEC).<sup>3</sup> It can be classified into 4 stages under a thermal cycle. At the Stage I, a temperature gradient is applied, and the thermovoltage is built up between the two electrodes. This arises from the Soret effect of the ions, that is, the accumulations of the cations and anions at the cold and hot ends of the ionic material, respectively. The external load is disconnected. At the stage II, an external load is connected to the ITEC, electrons and holes flow from the external circuit to the two electrodes to balance the accumulated cations and anions there. At the stage III, the heater is turned off, and the external load is disconnected. While the accumulated cations and anions are retrieved, the electrons and holes remaining at the two electrodes generate a negative voltage. At the stage IV, the external load is reconnected to the ITEC again, the electrons and holes retrieve to the external load. As a result, the voltage gradually decreases to zero.

## References

1. Z. Guo, T. Sato, Y. Han, N. Takamura, R. Ikeda, T. Miyamoto, N. Kida, M. Ogino, Y. Takahashi, N. Kasuya, S. Watanabe, J. Takeya, Q. Wei, M. Mukaida and H. Okamoto, *Commun. Mater.*, 2024, **5**, 26.
2. D. M. DeLongchamp, B. D. Vogt, C. M. Brooks, K. Kano, J. Obrzut, C. A. Richter, O. A. Kirillov and E. K. Lin, *Langmuir*, 2005, **21**, 11480-11483.
3. Q. Qian, H. Cheng, H. Xie, Y. Wu, Y. Fang, Q. Le, S. Yue and J. Ouyang, *Adv. Energy Mater.*, 2025, **15**, 2404522.